Search for isotensor exotic meson and twist 4 contribution to $\gamma^*\gamma \to \rho\rho$

I.V. Anikin [a,b,c], B. Pire [b], O.V. Teryaev [c]

[a] *LPT, Université Paris-Sud, 91405 Orsay, France* [1]
[b] *CPHT, École Polytechnique, 91128 Palaiseau cedex, France* [2]
[c] *Bogoliubov Laboratory of Theoretical Physics, JINR, 141980 Dubna, Russia*

Received 4 July 2005; received in revised form 30 August 2005; accepted 31 August 2005

Available online 15 September 2005

Editor: N. Glover

Abstract

We present a theoretical estimate for the cross-section of exclusive $\rho^+\rho^-$ and $\rho^0\rho^0$-meson production in two photon collisions when one of the initial photons is highly virtual. We focus on the discussion of the twist 4 contributions which are related to the production of an exotic isospin 2 resonance of two ρ mesons. Our analysis shows that the recent experimental data obtained by the L3 Collaboration at LEP can be understood as a signal for the existence of an exotic isotensor resonance with a mass around 1.5 GeV.

© 2005 Elsevier B.V. Open access under CC BY license.

1. Introduction

Exclusive reactions $\gamma^*\gamma \to A + B$ which may be accessed in e^+e^- collisions have been shown [1] to have a partonic interpretation in the kinematical region of large virtuality of one photon and of small center of mass energy. The scattering amplitude factorizes in a long distance dominated object—the generalized distribution amplitude (GDA)—and a short distance perturbatively calculable scattering matrix. A phenomenological analysis of the $\pi\pi$ channel [2] has shown that precise experimental data could be collected at intense e^+e^- collider experiments such as BaBar and Belle. Meanwhile, first data on the $\rho^0\rho^0$ channel at LEP have been published [3] and analyzed [4], showing the compatibility of the QCD leading order analysis with experiment at quite modest values of Q^2.

E-mail address: anikin@theor.jinr.ru (I.V. Anikin).

[1] Unité mixte 8627 du CNRS.
[2] Unité mixte 7644 du CNRS.

In this Letter, we focus on the comparison of processes $\gamma^*\gamma \to \rho^0\rho^0$ and $\gamma^*\gamma \to \rho^+\rho^-$ in the context of searching an exotic isospin 2 resonance decaying in two ρ mesons; such channels have recently been studied at LEP by the L3 Collaboration [3,5]. A related study for photoproduction [6] raised the problem of $\rho^0\rho^0$ enhancement with respect to $\rho^+\rho^-$ at low energies. One of the solutions of this problem was based on the prediction [7] and further exploration [8] of the possible existence of isotensor state, whose interference with the isoscalar state is constructive for neutral mesons and destructive for charged ones. This option was also independently considered in [9]. The crucial property of such an exotic state is the absence of $\bar{q}q$ wave function at any momentum resolution. In other words, quark–antiquark component is absent both in its non-relativistic description and at the level of the light-cone distribution amplitude. This is by no means common: for instance, the 1^{-+} state which is a quark–gluon hybrid at the non-relativistic level is described by a leading twist quark–antiquark distribution amplitude [10]. Contrary to that, an isotensor state on the light cone corresponds to the twist 4 or higher and its contribution is thus power suppressed at large Q^2. This is supported by the mentioned L3 data, where the high Q^2 ratio two of the cross sections of charged and neutral mesons production points out an isoscalar state.

We studied both perturbative and non-perturbative ingredients of QCD factorization for the description of an isotensor state. Namely, we calculated the twist 4 coefficient function and extracted the non-perturbative matrix elements from L3 data. Our analysis is compatible with the existence of an isotensor exotic meson with a mass around 1.5 GeV.

2. Amplitude of $\gamma^*\gamma \to \rho\rho$ process

The reaction which we study here is $e(k) + e(l) \to e(k') + e(l') + \rho(p_1) + \rho(p_2)$, where ρ stands for the triplet ρ mesons; the initial electron $e(k)$ radiates a hard virtual photon with momentum $q = k - k'$, with $q^2 = -Q^2$ quite large. This means that the scattered electron $e(k')$ is tagged. To describe the given reaction, it is useful to consider the subprocess $e(k) + \gamma(q') \to e(k') + \rho(p_1) + \rho(p_2)$. Regarding the other photon momentum $q' = l - l'$, we assume that, firstly, its momentum is almost collinear to the electron momentum l and, secondly, that q'^2 is approximately equal to zero, which is a usual approximation when the second lepton is untagged.

In two ρ meson production, we are interested in the channel where the resonance corresponds to the exotic isospin, i.e., $I = 2$, and usual J^{PC} quantum numbers. The J^{PC} quantum numbers are not essential for our study. Because the isospin 2 has only a projection on the four quark correlators, the study of mesons with the isospin 2 can help to throw light upon the four quark states. We thus, together with the mentioned reactions, study the following processes: $e(k) + e(l) \to e(k') + e(l') + R(p)$ and $e(k) + \gamma(q') \to e(k') + R(p)$, where meson $R(p)$ possesses isospin $I = 2$.

Considering the amplitude of the $\gamma^*\gamma$ subprocess, we write

$$\mathcal{A}_{(i,j)}\big(\gamma\gamma^* \to \rho\rho\big) = \varepsilon'^{(i)}_\mu \varepsilon^{(j)}_\nu \int d^4z_1\, d^4z_2\, e^{-iq'\cdot z_1 - iq\cdot z_2}\langle\rho(p_1)\rho(p_2)\big|T\big[J_\mu(z_1)J_\nu(z_2)\big]\big|0\rangle, \tag{1}$$

where J_μ denotes the quark electromagnetic current $J_\mu = \bar{\psi}\mathcal{Q}\gamma_\mu\psi$ with the charge matrix $\mathcal{Q}$ belonging to $SU_F(2)$ group. The photon polarization vectors read

$$\varepsilon'^{(\pm)}_\mu = \left(0, \frac{\mp 1}{\sqrt{2}}, \frac{+i}{\sqrt{2}}, 0\right), \qquad \varepsilon^{(\pm)}_\mu = \left(0, \frac{\mp 1}{\sqrt{2}}, \frac{-i}{\sqrt{2}}, 0\right), \qquad \varepsilon^{(0)}_\mu = \left(\frac{|q|}{\sqrt{Q^2}}, 0, 0, \frac{q_0}{\sqrt{Q^2}}\right), \tag{2}$$

for the real and virtual photons, respectively. The coefficient functions of twist 2 operators to operator product expansion of currents product in (1) were discussed in detail in [4], while the contributions of new twist 4 operators are described by coefficient functions calculated long ago in [11] when considering the problem of twist 4 corrections to deep inelastic scattering.

Let us now turn on the flavour or isospin structure of the corresponding amplitudes. The $\rho\rho$ state with $I = 0$ can be projected on both the two and four quark operators, while the state with $I = 2$ on the four quark operator only.

Indeed, let us start from the consideration of the vacuum-to-$\rho\rho$ matrix element in (1)

$$\langle \rho^a \rho^b | \bar{\psi}_f(0) \Gamma \psi_g(z) | 0 \rangle = \delta^{ab} I_{fg} \Phi^{I=0} + i \varepsilon^{abc} \tau_{fg}^c \Phi^{I=1}, \tag{3}$$

where the quark fields are shown with free flavour indices and Γ stands for the corresponding γ-matrix. The isoscalar and isovector GDAs Φ^I in (3) are well known, see for instance [12]. Note that, in (3), the correspondence between triplets $\{\rho^1, \rho^2, \rho^3\}$ and $\{\rho^+, \rho^-, \rho^0\}$ is given by the standard way.

Moreover, for the coefficient function at higher order in the strong coupling constant, the corresponding matrix element gives us

$$\langle \rho^a \rho^b | [\bar{\psi}_{f_1}(0) \Gamma_1 \psi_{g_1}(\eta)][\bar{\psi}_{f_2}(z) \Gamma_2 \psi_{g_2}(\xi)] | 0 \rangle. \tag{4}$$

Using the Clebsch–Gordan decomposition, we obtain

$$\left([\bar{\psi}_{f_1} \psi_{g_1}][\bar{\psi}_{f_2} \psi_{g_2}]\right)^{I=0, I_z=0} \quad \Rightarrow \quad -\frac{1}{\sqrt{3}}\left[\frac{1}{2}\tau_{f_1 g_1}^0 \tau_{f_2 g_2}^0 + \tau_{f_1 g_1}^+ \tau_{f_2 g_2}^- + \tau_{f_1 g_1}^- \tau_{f_2 g_2}^+\right]\tilde{\Phi}^{I=0, I_z=0} \tag{5}$$

for the isospin 0 and $I_z = 0$ projection of the four quark operator in (4), and

$$\left([\bar{\psi}_{f_1} \psi_{g_1}][\bar{\psi}_{f_2} \psi_{g_2}]\right)^{I=2, I_z=0} \quad \Rightarrow \quad \frac{1}{\sqrt{6}}\left[\tau_{f_1 g_1}^0 \tau_{f_2 g_2}^0 - \tau_{f_1 g_1}^+ \tau_{f_2 g_2}^- - \tau_{f_1 g_1}^- \tau_{f_2 g_2}^+\right]\tilde{\Phi}^{I=2, I_z=0} \tag{6}$$

for the isospin 2 and $I_z = 0$ projection of the four quark operator in (4). The four quark GDAs $\tilde{\Phi}^{I, I_z=0}$ can be defined in an analogous manner as the two quark GDAs. Hence, one can see that the amplitudes (1) for $\rho^0\rho^0$ and $\rho^+\rho^-$ productions can be written in the form of the decomposition:

$$\mathcal{A}_{(+,+)} = \mathcal{A}_{(+,+)2}^{I=0, I_z=0} + \mathcal{A}_{(+,+)4}^{I=0, I_z=0} + \mathcal{A}_{(+,+)4}^{I=2, I_z=0}, \tag{7}$$

where the subscripts 2 and 4 in the amplitudes imply that the given amplitudes are associated with the two and four quark correlators, respectively. The amplitudes corresponding to $\rho^+\rho^-$ production are not independent and can be expressed through the corresponding amplitudes of $\rho^0\rho^0$ production. Indeed, one can derive the following relations:

$$\mathcal{A}_{(+,+)k}^{I=0, I_z=0}(\gamma\gamma^* \to \rho^+\rho^-) = \mathcal{A}_{(+,+)k}^{I=0, I_z=0}(\gamma\gamma^* \to \rho^0\rho^0) \quad \text{for } k = 2, 4,$$

$$\mathcal{A}_{(+,+)4}^{I=2, I_z=0}(\gamma\gamma^* \to \rho^+\rho^-) = -\frac{1}{2}\mathcal{A}_{(+,+)4}^{I=2, I_z=0}(\gamma\gamma^* \to \rho^0\rho^0). \tag{8}$$

The amplitude of two ρ meson production in two photon collision can be also presented through a resonant intermediate state. The vacuum to $\rho\rho$ matrix element in the r.h.s. of (1) can be traded for

$$\sum_{I=0,1,2} \langle \rho(p_1)\rho(p_2) | R^I(p) \rangle \frac{1}{M_{R^I}^2 - p^2 - i\Gamma_{R^I} M_{R^I}} \langle R^I(p) | T[J_\mu(0) J_\nu(z)] | 0 \rangle, \tag{9}$$

where $R^I(p)$ is the resonance with three possible isospin $I = 0, 1, 2$. Note that, in our case, only isospin 0 and 2 cases are relevant due to the positive C-parity of the initial and final states. The matrix element $\langle \rho\rho | R^I \rangle$ defines the corresponding coupling constant of meson and $\langle R^I | T[J_\mu(0) J_\nu(z)] | 0 \rangle$ is considered up to the second order of strong coupling constant α_S, i.e., this matrix element is written as a sum of two- and four-quark correlators.

3. Differential cross sections

Previously, the theoretical description of the experimental data collected for the $\rho^0\rho^0$ production has been performed in [4]. Now, the subject of our study is the differential cross section corresponding to both the $\rho^0\rho^0$ and $\rho^+\rho^-$ productions in the electron–positron collision.

Using the equivalent photon approximation [13] we find the expression for the corresponding cross section:

$$\frac{d\sigma_{ee\to ee\rho\rho}}{dQ^2\,dW^2} = \int \cdots \int d\cos\theta\,d\phi\,dx_2\,\frac{\alpha}{\pi}F_{WW}(x_2)\frac{d\sigma_{e\gamma\to e\rho\rho}}{dQ^2\,dW^2\,d\cos\theta\,d\phi}, \tag{10}$$

where the usual Weizsacker–Williams function F_{WW} is used. In (10), the cross section for the subprocess reads

$$\frac{d\sigma_{e\gamma\to e\rho\rho}}{dQ^2\,dW^2\,d\cos\theta\,d\phi} = \frac{\alpha^3}{16\pi}\frac{\beta}{S_{e\gamma}^2}\frac{1}{Q^2}\left(1 - \frac{2S_{e\gamma}(Q^2+W^2-S_{e\gamma})}{(Q^2+W^2)^2}\right)\left|A_{(+,+)}\right|^2, \tag{11}$$

where the amplitude $A_{(+,+)}$ is defined by (7). For the case of $\rho^0\rho^0$ production, the cross section (10) takes the form:

$$\begin{aligned}
\frac{d\sigma_{ee\to ee\rho^0\rho^0}}{dQ^2\,dW^2} &= \frac{100\alpha^4}{9}G\big(S_{ee},Q^2,W^2\big)\beta \\
&\quad \times \Bigg(\frac{\Gamma_{R^0}M_{R^0}}{\beta_0((M_{R^0}^2-W^2)^2+\Gamma_{R^0}^2M_{R^0}^2)}\left[\mathbf{S}_2^{I=0,I_3=0} + \frac{\alpha_S(Q^2)M_{R^0}^2}{Q^2}\mathbf{S}_4^{I=0,I_3=0}\right]^2 \\
&\quad + \frac{\Gamma_{R^2}M_{R^2}}{\beta_2((M_{R^2}^2-W^2)^2+\Gamma_{R^2}^2M_{R^2}^2)}\left[\frac{\alpha_S(Q^2)M_{R^2}^2}{Q^2}\mathbf{S}_4^{I=2,I_3=0}\right]^2 \\
&\quad + 2\sqrt{\frac{\Gamma_{R^0}\Gamma_{R^2}M_{R^0}M_{R^2}}{\beta_0\beta_2}}\frac{(M_{R^0}^2-W^2)(M_{R^2}^2-W^2)+(\Gamma_{R^0}M_{R^0})(\Gamma_{R^2}M_{R^2})}{((M_{R^0}^2-W^2)^2+\Gamma_{R^0}^2M_{R^0}^2)((M_{R^2}^2-W^2)^2+\Gamma_{R^2}^2M_{R^2}^2)} \\
&\quad \times \left[\mathbf{S}_2^{I=0,I_3=0} + \frac{\alpha_S(Q^2)M_{R^0}^2}{Q^2}\mathbf{S}_4^{I=0,I_3=0}\right]\frac{\alpha_S(Q^2)M_{R^2}^2}{Q^2}\mathbf{S}_4^{I=2,I_3=0}\Bigg),
\end{aligned} \tag{12}$$

where Γ_{R^I} stand for the total widths. The dimensionful structure constants $\mathbf{S}_4^{I,I_3=0}$ and $\mathbf{S}_2^{I=0,I_3=0}$ are related to the nonperturbative vacuum-to-meson matrix elements. The β-functions are also defines in the standard ways: $\beta = \sqrt{1-4m_\rho^2/W^2}$ and $\beta_I = \sqrt{1-4m_\rho^2/M_{R^I}^2}$. The function G in (12) is equal to

$$G\big(S_{ee},Q^2,W^2\big) = \int\limits_0^1 dx_2\,F_{WW}(x_2)\left[\frac{1}{x_2^2 S_{ee}^2 Q^2} - \frac{2}{x_2 S_{ee} Q^2(Q^2+W^2)} + \frac{2}{Q^2(Q^2+W^2)^2}\right]. \tag{13}$$

The differential cross section corresponding to $\rho^+\rho^-$ production can be obtained using (8), we have

$$\begin{aligned}
\frac{d\sigma_{ee\to ee\rho^+\rho^-}}{dQ^2\,dW^2} &= \frac{200\alpha^4}{9}G\big(S_{ee},Q^2,W^2\big)\beta \\
&\quad \times \Bigg(\frac{\Gamma_{R^0}M_{R^0}}{\beta_0((M_{R^0}^2-W^2)^2+\Gamma_{R^0}^2M_{R^0}^2)}\left[\mathbf{S}_2^{I=0,I_3=0} + \frac{\alpha_S(Q^2)M_{R^0}^2}{Q^2}\mathbf{S}_4^{I=0,I_3=0}\right]^2 \\
&\quad + \frac{1}{4}\frac{\Gamma_{R^2}M_{R^2}}{\beta_2((M_{R^2}^2-W^2)^2+\Gamma_{R^2}^2M_{R^2}^2)}\left[\frac{\alpha_S(Q^2)M_{R^2}^2}{Q^2}\mathbf{S}_4^{I=2,I_3=0}\right]^2 \\
&\quad - \sqrt{\frac{\Gamma_{R^0}\Gamma_{R^2}M_{R^0}M_{R^2}}{\beta_0\beta_2}}\frac{(M_{R^0}^2-W^2)(M_{R^2}^2-W^2)+(\Gamma_{R^0}M_{R^0})(\Gamma_{R^2}M_{R^2})}{((M_{R^0}^2-W^2)^2+\Gamma_{R^0}^2M_{R^0}^2)((M_{R^2}^2-W^2)^2+\Gamma_{R^2}^2M_{R^2}^2)} \\
&\quad \times \left[\mathbf{S}_2^{I=0,I_3=0} + \frac{\alpha_S(Q^2)M_{R^0}^2}{Q^2}\mathbf{S}_4^{I=0,I_3=0}\right]\frac{\alpha_S(Q^2)M_{R^2}^2}{Q^2}\mathbf{S}_4^{I=2,I_3=0}\Bigg).
\end{aligned} \tag{14}$$

Note that we have explicitly separated out, in (12) and (14), the running coupling constant $\alpha_S(Q^2)$ which appears in the twist 4 terms. Because of we will study the Q^2 dependence of the corresponding cross sections at rather small values of Q^2, we use the Shirkov and Solovtsov's analytical approach [14] to determine the running coupling constant in the region of small Q^2. Detailed discussion on different aspects of using the analytical running coupling constant may be found in [10,16] and references therein.

4. LEP data fitting

In the previous section we derived the differential cross sections $d\sigma_{ee\to ee\rho\rho}/dQ^2\,dW^2$ for both the $\rho^0\rho^0$ and $\rho^+\rho^-$ channels, based on the QCD analysis. These expressions contain a number of unknown phenomenological parameters, which are intrinsically related to non perturbative quantities encoded in the generalized distribution amplitudes. One should now make a fit of these phenomenological parameters in order to get a good description of experimental data. The best values of the parameters can be found by the method of least squares, χ^2-method, which flows from the maximum likelihood theorem, but we postpone a comprehensive χ^2-analysis to a forth-coming more detailed paper. Here, we implement a naive fitting analysis to get an acceptable agreement with the experimental data. Thus, we have the following set of parameters for fitting:

$$\mathbf{P} = \big\{ M_{R^0}, \Gamma_{R^0}, M_{R^2}, \Gamma_{R^2}, \mathbf{S}_2^{I=0,I_3=0}, \mathbf{S}_4^{I=0,I_3=0}, \mathbf{S}_4^{I=2,I_3=0} \big\}. \tag{15}$$

We start with the study of the W dependence of the cross sections. For this goal, following the papers [3,5], we determine the cross section of process $ee \to ee\rho\rho$ normalized by the integrated luminosity function:

$$\sigma_{\gamma\gamma^*}\big(\langle W\rangle\big) = \frac{\int dQ^2\,\mathcal{L}(Q^2, \langle W\rangle)\sigma_{\gamma\gamma^*}(Q^2, \langle W\rangle)}{\int dQ^2\,\mathcal{L}(Q^2, \langle W\rangle)}, \tag{16}$$

where the definition of the luminosity function $\mathcal{L}$ is taken from [15]. The value $\langle W\rangle$ corresponds to the center of each bin, see [3,5]. Focusing first on the region of larger Q^2 we fit the parameters associated with the dominant contribution which comes from the twist 2 term amplitude, which is associated with the non-exotic resonance (or background) with isospin $I = 0$.

Generally speaking, there are many isoscalar resonances with masses in the region of 1–3 GeV. To include their total effect we introduce a mass and width for an "effective" isoscalar resonance. We also checked that varying the phase of this "effective" resonance, whose value is ambiguous, produces a variation smaller than 20% at low Q^2, which is compatible to the expected error in the determination of non-perturbative matrix elements.

We then determine the values of the mass and width by fitting the data for the region of larger Q^2 (i.e., when Q^2 is in the interval $1.2 < Q^2 < 8.5$ GeV^2). We thus can fix the parameters $\mathbf{S}_2^{I=0,I_3=0}$, M_{R^0} and Γ_{R^0}. Good agreement can be achieved with $M_{R^0} = 1.8$ GeV, $\Gamma_{R^0} = 1.00$ GeV and $\mathbf{S}_2^{I=0,I_3=0}$ within the interval $(0.12, 0.16)$. As can be expected the width of the effective isoscalar "resonance" is fairly large. It means that we actually deal with a non-resonant background.

Next, we fit the W-dependence of the cross section for small values of Q^2, i.e., $0.2 < Q^2 < 0.85$ GeV^2. In this region all twist contributions may be important. We find that the experimental data can be described by the following choice of the parameters: $M_{R^2} = 1.5$ GeV, $\Gamma_{R^2} = 0.4$ GeV while the parameters $\mathbf{S}_4^{I=0,I_3=0}$ and $\mathbf{S}_4^{I=2,I_3=0}$ are in the intervals $(0.002, 0.006)$ and $(0.012, 0.018)$, respectively.

Further, we include in our analysis the Q^2 dependence of $\rho^0\rho^0$ and $\rho^+\rho^-$ production cross sections, i.e., $d\sigma_{ee\to ee\rho\rho}/dQ^2$, which should fix the remaining arbitrariness of the parameters. We finally find that the best description of both W and Q^2 dependence is reached at

$$\begin{aligned} & M_{R^2} = 1.5\text{ GeV}, \qquad \Gamma_{R^2} = 0.4\text{ GeV}, \\ & \mathbf{S}_2^{I=0,I_3=0} = 0.12\text{ GeV}, \qquad \mathbf{S}_4^{I=0,I_3=0} = 0.006\text{ GeV}, \qquad \mathbf{S}_4^{I=2,I_3=0} = 0.018\text{ GeV}. \end{aligned} \tag{17}$$
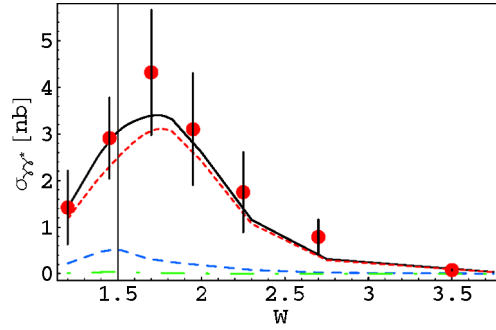
Fig. 1. W dependence of the cross section $\sigma_{ee \to ee\rho^0\rho^0}$ normalized by the integrated luminosity function, in the $1.2 < Q^2 < 8.5$ region. The short-dashed line corresponds to the leading twist 2 contribution; the dash-dotted line to the twist 4 contribution; the middle-dashed line to the interference of twist 2 and 4 contributions. The solid line corresponds to the sum of all contributions.
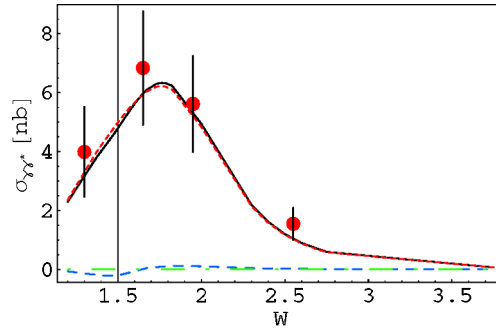

Fig. 2. W dependence of the cross section $\sigma_{ee \to ee\rho^+\rho^-}$ with the same conventions as for Fig. 1.

Note that these rather small values of twist 4 structure constants $\mathbf{S}_4$ compared to the twist 2 structure constant $\mathbf{S}_2$ indicate that leading twist contribution dominate for the values Q^2 around or greater than 1 GeV^2. This should be compared with what was obtained in a particular renormalon model in [17].

We stress that our result supports the smallness of genuine higher twist at hadronic scale, previously found in studies of genuine twist 3 contribution to structure function g_2 [18]. One may think that the relative size of the twist 4 coefficients is unnaturally small. This is in part due to our parametrization which factors M_R^2 in front of our factors $\mathbf{S}_4$. If we replace M_R by $\Lambda_{\mathrm{QCD}} \sim 0.3$ GeV, we get $\mathbf{S}_4^{I=0} = 0.22$ GeV and $\mathbf{S}_4^{I=2} = 0.45$ GeV and all constants $\mathbf{S}_4^{I=0}$, $\mathbf{S}_4^{I=2}$ and $\mathbf{S}_2^{I=0}$ become of the same order, which may look more natural.

Our theoretical description of the LEP experimental data are presented on Figs. 1–5. The plots depicted on Figs. 1–4 have the following notations: the short-dashed line corresponds to the contribution coming from the leading twist term of (12); the dash-dotted line—to the contribution from the twist 4 term of (12); the middle-dashed line—to the contributions from the interference between twist 2 and twist 4 terms of (12) and (14); the long-dashed line—to the contribution from the interference between isoscalar and isotensor terms. Finally the solid line corresponds to the sum of all contributions. On Fig. 5, we present the LEP data and our theoretical curves for both the $\rho^0\rho^0$ and $\rho^+\rho^-$ production differential cross sections as functions of Q^2. The solid line on Fig. 5 corresponds to the $\rho^0\rho^0$ differential cross section while the dashed one—to the $\rho^+\rho^-$ differential cross section.
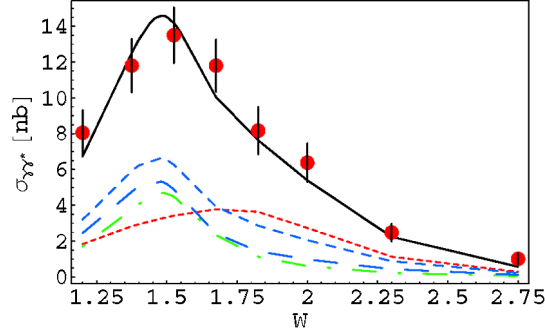
Fig. 3. *W* dependence of the cross section $\sigma_{ee \to ee\rho^0\rho^0}$ normalized by the integrated luminosity function in the $0.2 < Q^2 < 0.85$ region. The short-dashed line corresponds to the leading twist 2 contribution; the dash-dotted line to the twist 4 contribution; the middle-dashed line to the contributions from the interference between twist 2 and twist 4 terms; the long-dashed line to the contribution from the interference between isoscalar and isotensor terms. The solid line corresponds to the sum of all contributions.
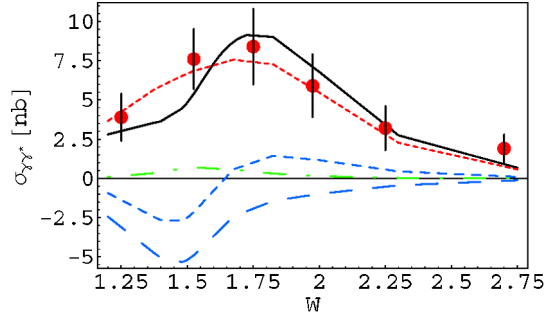

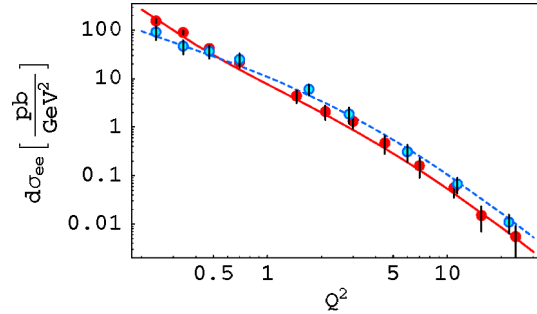Fig. 4. same as Fig. 3 for the cross section $\sigma_{ee \to ee\rho^+\rho^-}$ in the $0.2 < Q^2 < 0.85$ region.

Fig. 5. The Q^2 dependence of the differential cross sections $d\sigma_{ee \to ee\rho^0\rho^0}/dQ^2$ and $d\sigma_{ee \to ee\rho^+\rho^-}/dQ^2$. The solid line corresponds to the case of $\rho^0\rho^0$ production; the dashed line to the case of $\rho^+\rho^-$ production.

5. Discussions and conclusions

The fitting of LEP data based on the QCD factorization of the amplitude into a hard subprocess and a generalized distribution amplitude is thus consistent with the existence of an isospin $I = 2$ exotic meson [7–9,19] with a mass in the vicinity of 1.5 GeV and a width around 0.4 GeV. The contributions of such an exotic meson in the two ρ meson production cross sections (see, (12) and (14)) are directly associated with some twist 4 terms that we

have identified. At large Q^2, these twist 4 contributions become negligible and the behaviours of the $\rho^0\rho^0$ and $\rho^+\rho^-$ cross sections are controlled by the leading twist 2 contributions, see Figs. 1 and 2. Figs. 3 and 4 show the increasing role of higher twist contributions when decreasing Q^2. Namely, the interference between twist 2 and 4 amplitudes gives the dominant contributions to $\rho^0\rho^0$ production in the lower Q^2 interval, and is thus responsible of the W dependence of the cross section in these kinematics. In particular, in this interference term the main contribution arises from the interference between isoscalar and isotensor structures, see the long-dashed lines on Figs. 3 and 4.

Analysing the Q^2 dependence, we can see that due to the presence of a twist 4 amplitude and its interference with the leading twist 2 component, the $\rho^0\rho^0$ cross section at small Q^2 is a few times higher than the $\rho^+\rho^-$ cross section, see Fig. 5. While for the region of large Q^2 where any higher twist effects are negligible the $\rho^0\rho^0$ cross section is less than the $\rho^+\rho^-$ cross section by the factor 2, which is typical from an isosinglet channel (see also (12) and (14)).

The reaction $\gamma^*\gamma \to \rho\rho$ and its QCD analysis in the framework of Ref. [1] thus proves its efficiency to reveal facts on hadronic physics which would remain quite difficult to explain in a quantitative way otherwise. The leading twist dominance is seen to persist down to values of Q^2 around 1 GeV^2. Other aspects of QCD may be revealed in different kinematical regimes through the same reaction [20]. Its detailed experimental analysis at intense electron colliders within the BaBar and Belle experiments is thus extremely promising. Data at higher energies in a future linear collider should also be foreseen.

Note that the non-perturbative calculations of the relevant $I = 2$ twist 4 matrix elements also deserve special interest. In particular, one may follow the ideas developed for pion distribution [21] which allowed to relate higher and lower twists in multicolour QCD. The generalization for the case of ρ mesons, anticipated by the authors of [21], and use of crossing relations between various kinematical domains provided by Radon transform technique [22] may allow to apply these result in the case under consideration.

In conclusion, let us stress that the L3 data allows to estimate the contribution of higher twist four quark light cone distribution to the production amplitude of vector meson pairs. Our numerical analysis leads to a rather small width for the corresponding resonant state, which is nothing else as an exotic four-quark isotensor meson. At the same time, a more elaborate experimental, theoretical and numerical analysis is required to confirm, with better accuracy, the smallness of the width and the existence of an exotic meson.

Acknowledgements

References

[1] M. Diehl, T. Gousset, B. Pire, O.V. Teryaev, Phys. Rev. Lett. 81 (1998) 1782, hep-ph/9805380;
   M. Diehl, T. Gousset, B. Pire, Nucl. Phys. B (Proc. Suppl.) 82 (2000) 322, hep-ph/9907453.
[2] M. Diehl, T. Gousset, B. Pire, Phys. Rev. D 62 (2000) 073014, hep-ph/0003233.
[3] L3 Collaboration, P. Achard, et al., Phys. Lett. B 568 (2003) 11.
[4] I.V. Anikin, B. Pire, O.V. Teryaev, Phys. Rev. D 69 (2004) 014018, hep-ph/0307059.
[5] L3 Collaboration, P. Achard, et al., Phys. Lett. B 597 (2004) 26;
   L3 Collaboration, P. Achard, et al., Phys. Lett. B 604 (2004) 48;
   L3 Collaboration, P. Achard, et al., Phys. Lett. B 615 (2005) 19.

[6] J.L. Rosner, Phys. Rev. D 70 (2004) 034028, hep-ph/0404245.
[7] N.N. Achasov, S.A. Devyanin, G.N. Shestakov, Phys. Lett. B 108 (1982) 134;
    N.N. Achasov, S.A. Devyanin, G.N. Shestakov, Z. Phys. C 16 (1982) 55.
[8] N.N. Achasov, S.A. Devyanin, G.N. Shestakov, Z. Phys. C 27 (1985) 99;
    N.N. Achasov, G.N. Shestakov, Sov. Phys. Usp. 34 (1991) 471, Usp. Fiz. Nauk 161 (1991) 53.
[9] B.A. Li, K.F. Liu, Phys. Lett. B 118 (1982) 435;
    B.A. Li, K.F. Liu, Phys. Rev. Lett. 51 (1983) 1510;
    B.A. Li, K.F. Liu, Phys. Rev. D 28 (1983) 1636;
    B.A. Li, K.F. Liu, Phys. Rev. D 30 (1984) 613.
[10] I.V. Anikin, B. Pire, L. Szymanowski, O.V. Teryaev, S. Wallon, Phys. Rev. D 71 (2005) 034021, hep-ph/0411407;
    I.V. Anikin, B. Pire, L. Szymanowski, O.V. Teryaev, S. Wallon, Phys. Rev. D 70 (2004) 011501, hep-ph/0401130.
[11] R.L. Jaffe, M. Soldate, Phys. Rev. D 26 (1982) 49.
[12] M. Diehl, Phys. Rep. 388 (2003) 41, hep-ph/0307382.
[13] V.M. Budnev, I.F. Ginzburg, G.V. Meledin, V.G. Serbo, Phys. Rep. 15 (1974) 181.
[14] D.V. Shirkov, I.L. Solovtsov, Phys. Rev. Lett. 79 (1997) 1209.
[15] J.H. Field, Nucl. Phys. B 168 (1980) 477.
[16] A.P. Bakulev, K. Passek-Kumericki, W. Schroers, N.G. Stefanis, Phys. Rev. D 70 (2004) 033014, hep-ph/0405062;
    A.P. Bakulev, K. Passek-Kumericki, W. Schroers, N.G. Stefanis, Phys. Rev. D 70 (2004) 079906, Erratum.
[17] S.S. Agaev, M. Guidal, B. Pire, Eur. Phys. J. C 37 (2004) 457, hep-ph/0403266;
    J.R. Andersen, Phys. Lett. B 475 (2000) 141, hep-ph/9909396.
[18] E155 Collaboration, P.L. Anthony, et al., hep-ex/0204028;
    Jefferson Lab Hall A Collaboration, X. Zheng, et al., Phys. Rev. C 70 (2004) 065207, nucl-ex/0405006.
[19] L. Maiani, F. Piccinini, A.D. Polosa, V. Riquer, AIP Conf. Proc. 756 (2005) 321, hep-ph/0501077.
[20] B. Pire, L. Szymanowski, S. Wallon, hep-ph/0501155, hep-ph/0410108;
    B. Pire, L. Szymanowski, Phys. Rev. D 71 (2005) 111501;
    R. Enberg, B. Pire, L. Szymanowski, S. Wallon, hep-ph/0508134.
[21] N.Y. Lee, P.V. Pobylitsa, M.V. Polyakov, K. Goeke, J. Phys. G 27 (2001) L127, hep-ph/0011166.
[22] O.V. Teryaev, Phys. Lett. B 510 (2001) 125, hep-ph/0102303.